THE ARCHIVE OF MECHANICAL ENGINEERING

VOL. LX 2013 Number 1

10.2478/meceng-2013-0004

Key words: multibody dynamics, gears, involute gears, beveloid gears, contact forces, elastic multibody system

TRONG PHU DO[*], *PASCAL ZIEGLER*[*], *PETER EBERHARD*[*]

SIMULATION OF ELASTIC GEARS WITH NON-STANDARD FLANK PROFILES

There exist cases where precise simulations of contact forces do not allow modeling the gears as rigid bodies but a fully elastic description is needed. In this paper, a modally reduced elastic multibody system including gear contact based on a floating frame of reference formulation is proposed that allows very precise simulations of fully elastic gears with appropriately meshed gears in reasonable time even for many rotations. One advantage of this approach is that there is no assumption about the geometry of the gears and, therefore, it allows precise investigations of contacts between gears with almost arbitrary non-standard tooth geometries including flank profile corrections.

This study presents simulation results that show how this modal approach can be used to efficiently investigate the interaction between elastic deformations and flank profile corrections as well as their influence on the contact forces. It is shown that the elastic approach is able to describe important phenomena like early addendum contact for insufficiently corrected profiles in dependence of the transmitted load. Furthermore, it is shown how this approach can be used for precise and efficient simulations of beveloid gears.

1. Introduction

In many technical systems, very precise simulations of contact forces between gears require a fully elastic description, see [3] and [4]. This is particularly true for gears with very compliable gear bodies or for gears subject to high contact forces. A common way to model body flexibility is the finite element (FE) method. Unfortunately, the simulation of fully elastic gears still introduces many difficulties. First, for elastic bodies the use of an analytical collision detection is impossible, since contact surfaces depend on

[*] *Institute of Engineering and Computational Mechanics, University of Stuttgart, Pfaffenwaldring 9, 70569 Stuttgart, Germany; E-mail: [trongphu.do, pascal.ziegler, peter.eberhard]@itm.uni-stuttgart.de*

the elastic deformation. Furthermore, it is normally preferred for gear pairs to avoid common divisors in the number of teeth in order to reduce wear of the flanks. This results in a very high number of different possible contact pairs when the investigation of full rotations is necessary. Moreover, the enormous number of degrees of freedom for a system of adequately meshed gears renders a FE analysis of even a few rotations practically impossible. In order to reduce the number of nodal FE degrees of freedom and to increase computational efficiency, some sorts of model reduction technique are usually applied, see [6].

In [4], a modally reduced elastic multibody model including contact is presented. For the contact calculation a node-to-segment penalty formulation and a coarse collision detection are introduced and are integrated using an explicit time integration scheme. The algorithm and formulation making it possible to calculate contact forces of the work are applied in this study for the gears with non-standard flank profiles.

One technically very important application for non-standard flank profiles are beveloid gears, also known as conical involute gears. Nowadays, progress in the design and production of beveloid gears enables their use in an increasingly wide range of applications. The most familiar application of beveloid gears is the reduction gear used in marine transmissions. Since beveloid gears allow a certain amount of down angle, an optimal placement of the engine is possible. The down angle is achieved by a linearly changing profile shift of the involute profile across the width of the teeth, leading to a very complex tooth shape, see Figure 13. The contact stresses of a straight and a helical beveloid gear pair are introduced in [8] and [10], but the analyses are established only by an FE model of one pair of contact teeth of the gear pairs with a relatively small contact area. A straight beveloid gear pair will be studied in this work, followed by a simulation of the whole model with very large rotational angle and the effect of complex flank profiles on kinematic and dynamical interaction will be investigated.

2. Elastic Mutibody Model

In this section, the description of gear wheels as elastic multibody models is introduced and the modal reduction is explained. The contact algorithm and some simulation results are given in the subsections. For a deeper description, we refer to [15] and [16].

To overcome the large integration times of the FE model while still having an accurate model, a modally reduced model is used in this work. Usually, the deformations of gears are small and can easily be described by linear theory. However, the main application of gears includes large rotations

which are nonlinear by nature. Otherwise, most reduction techniques are based on linear methods, see [1] and [17]. One way to apply linear reduction methods despite of the large rotations is to use a floating frame of reference formulation, described in detail in [15] and [16]. This method is specially well suited for problems with a large movement of the reference frame and only small elastic deformations.

The basic idea of the floating frame of reference is the separation of the overall motion of a single flexible body into a usually nonlinear motion of the reference frame and a linear elastic deformation with respect to the reference frame, see [6] and [15].

The equations of motion for a free elastic multibody system read as

$$\boldsymbol{M}(\boldsymbol{z}_F)\dot{\boldsymbol{z}}_{II} = \boldsymbol{h}_e(\boldsymbol{z}_F) + \boldsymbol{h}_\omega(\boldsymbol{v}, \boldsymbol{\omega}, \boldsymbol{z}_F, \dot{\boldsymbol{z}}_F) + \boldsymbol{h}_a, \tag{1}$$

$$\boldsymbol{z}_{II} = \begin{bmatrix} \boldsymbol{v} & \boldsymbol{\omega} & \dot{\boldsymbol{z}}_F \end{bmatrix}^T, \tag{2}$$

where $\boldsymbol{M} \in \mathbb{R}^{(6+n)\times(6+n)}$ is the mass matrix, $\boldsymbol{h}_\omega \in \mathbb{R}^{6+n}$ are generalized inertial forces, $\boldsymbol{h}_e \in \mathbb{R}^{6+n}$ are generalized internal forces, $\boldsymbol{v} \in \mathbb{R}^3$ and $\boldsymbol{\omega} \in \mathbb{R}^3$ are the translational and the rotational velocity of the reference system, respectively. The nodal displacements of the FE structure are denoted by $\boldsymbol{z}_F \in \mathbb{R}^n$, where n is the number of elastic degrees of freedom. All external forces and torques, including contact forces, are summarized in $\boldsymbol{h}_a$. The approach leads to $6 + n$ degrees of freedom per elastic body. For the description of the elastic part, most often a FE model is used. Although this allows a very precise geometrical discretization, this typically means a large number of elastic degrees of freedom. In order to reduce the number of degrees of freedom, modal reduction is applied.

Modal reduction

In general the linear equations of motion for a FE model read

$$\boldsymbol{M}_F\ddot{\boldsymbol{z}}_F + \boldsymbol{K}_F\boldsymbol{z}_F = \boldsymbol{h}_F, \tag{3}$$

where $\boldsymbol{z}_F \in \mathbb{R}^n$ is the vector of nodal displacements, $\boldsymbol{M}_F \in \mathbb{R}^{n\times n}$ is the global mass matrix, $\boldsymbol{K}_F \in \mathbb{R}^{n\times n}$ represents the stiffness matrix and $\boldsymbol{h}_F \in \mathbb{R}^n$ are the external forces. The matrices $\boldsymbol{M}_F$ and $\boldsymbol{K}_F$ are constant. Even though, many different model reduction techniques exist, see [6], the approach used in this study is the simple modal reduction. The basic idea of the modal formulation is to use a reduced basis of shape functions, defined by a small number of $m \ll n$ eigenvectors. The n nodal displacements $\boldsymbol{z}_F$ are approximated by the m shape functions $\boldsymbol{\Phi}_{red}$ and a vector $\boldsymbol{q}_{red}$ as

$$\boldsymbol{z}_F \approx \boldsymbol{\Phi}_{red}\boldsymbol{q}_{red}, \tag{4}$$

where $\boldsymbol{\Phi}_{red}$ is the modal matrix, comprised of the eigenmodes of the finite element structure and $\boldsymbol{q}_{red} \in \mathbb{R}^m$ are the reduced elastic coordinates. The eigenvalues ω_i and the associated eigenmodes $\boldsymbol{\varphi}_i$ are derived from solving the eigenvalue problem $(-\omega_i \boldsymbol{M}_F + \boldsymbol{K}_F)\boldsymbol{\varphi}_i = \boldsymbol{0}$. The eigenmodes are chosen mass-orthonormal which results in an identity matrix for the reduced mass matrix $\boldsymbol{M}_{F,red}$. The reduced stiffness matrix becomes a diagonal matrix $\boldsymbol{K}_{F,red} = \mathrm{diag}(\omega_1^2, \ldots, \omega_m^2)$.

The configuration of a flexible body is described using two sets of coordinates. First, the reference coordinates describing the global nonlinear motion of the body reference frame with respect to the inertial frame. Second, the elastic coordinates describing the elastic deformation with respect to the reference frame. Therefore, the transformation between the elastic, i.e. the modal coordinates, and nodal coordinates with respect to the inertial frame, reads as

$$\boldsymbol{\rho}^I = \boldsymbol{A}\left(\boldsymbol{\rho}^i + \boldsymbol{R} + \boldsymbol{u}^i\right) \text{ with } \boldsymbol{u}^i = \boldsymbol{\Phi}\boldsymbol{q}, \tag{5}$$

where $\boldsymbol{A}$ is the transformation matrix between the inertial system I and the reference frame i, $\boldsymbol{\rho}^i$ is the position of the body reference frame, $\boldsymbol{R}$ is the constant position representing the undeformed configuration and $\boldsymbol{u}^i$ is the elastic displacement of the flexible body.

2.1. Contact algorithm

To calculate the contact forces, a general node-to-surface approach is used, see [7]. During normal operation with large rotational angles each flank may come into contact with many different flanks of the opposed gear. A collision detection looping over all flanks would be possible, but is very expensive, since a transformation from modal coordinates to nodal coordinates for every flank node would be needed despite the fact that for geometrical reasons only a small number of flanks are in contact at the same time. To reduce the possible contact nodes, and thus the numerical cost for the transformation, a coarse collision detection is used, see [3].

Coarse collision detection

The coarse collision detection is based on index nodes. Each tooth of a gear is referenced by an index node that is located in the center of each tooth. The absolute positions of the index nodes are calculated in every integration step. The closest index node to the center of the opposite gear is determined and called the instantaneous center node. Based on this center node, a small number of teeth on the left and right are considered as possible contact candidates, see Figure 1.

The coarse collision detection reduces not only the number of possible contact nodes but also the size of the transformation matrix, which is needed

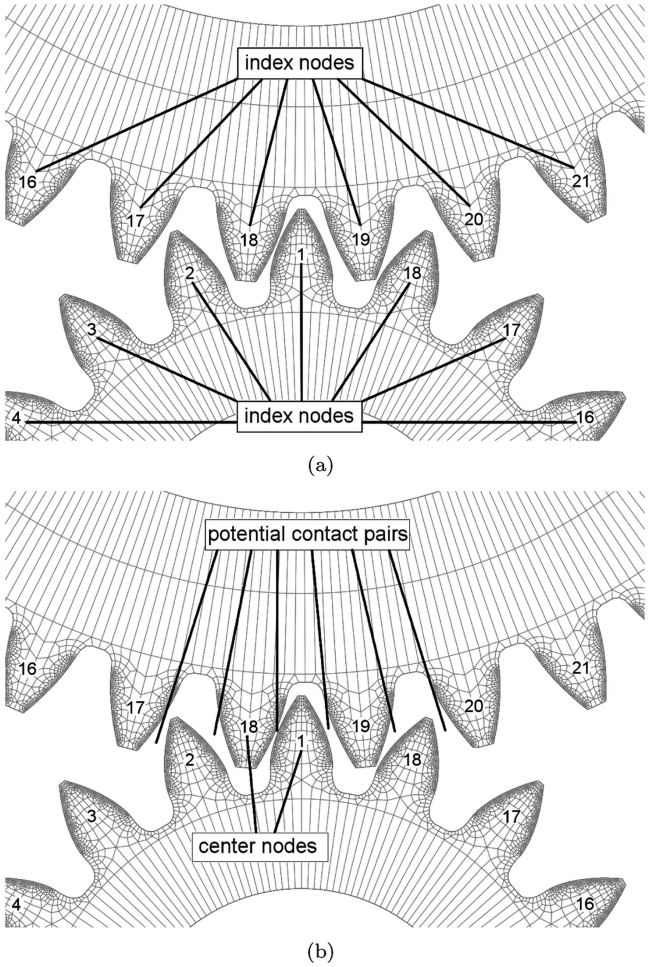

Fig. 1. Coarse contact detection using index nodes (a) and contact candidates (b)

to transform from modal coordinates to nodal coordinates. The transformation matrix is only updated if the center node changes. Therefore, in each integration step, only the index nodes and the currently valid transformation matrix of the contact candidates have to be stored in memory.

Fine collision detection

The contact between two flanks will be described using a fine collision detection based on a master/slave contact formulation. The two contact partners are separated into a master and a slave element. In a pure master/slave contact formulation, only the penetration of slave nodes into the master elements are considered. Therefore, the main task of the fine collision detection is to find the contact point of the slave node Q on the master surface $P_1P_2P_3P_4$ of the master element as shown in Figure 2.

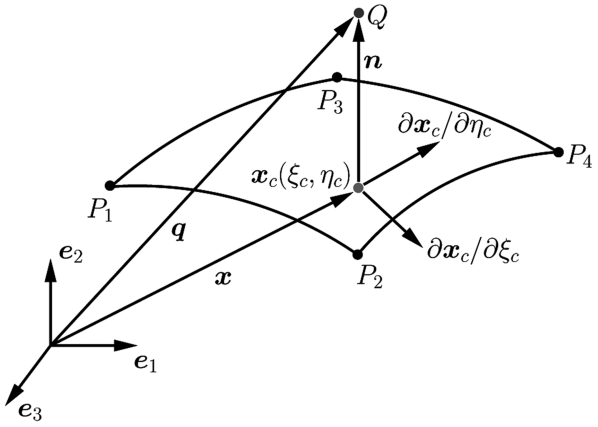

Fig. 2. Fine contact determination

By using linear hexahedral elements for the discretization of both contact partners, the shape function of the contact surfaces reads

$$\boldsymbol{x}(\xi,\eta) = \frac{1}{4}\sum_{i=1}^{4}(1+\xi_i\xi)\,(1+\eta_i\eta)\,\boldsymbol{z}_{F,i}, \qquad \xi_i,\eta_i \in [\pm 1]\,, \tag{6}$$

where ξ and η are parameters, ξ_i and η_i are element boundaries and $\boldsymbol{z}_{F,i}$ are node coordinates of the four master nodes.

Based on the node-to-surface contact, the contact point on the master surface can be found by solving the equations

$$\frac{\partial \boldsymbol{x}}{\partial \xi}^{T}(\xi_c,\eta_c)\,[\boldsymbol{q}-\boldsymbol{x}\,(\xi_c,\eta_c)] = 0, \tag{7}$$

$$\frac{\partial \boldsymbol{x}}{\partial \eta}^{T}(\xi_c,\eta_c)\,[\boldsymbol{q}-\boldsymbol{x}\,(\xi_c,\eta_c)] = 0. \tag{8}$$

A Newton-Raphson iteration is used to solve Equations (7) and (8). The penetration g_n of the slave node Q with coordinates $\boldsymbol{q}$ into the master surface is calculated as

$$g_n = \boldsymbol{n}^T\,(\boldsymbol{x}\,(\xi_c,\eta_c)-\boldsymbol{q}) \qquad \text{with } \boldsymbol{n} = \frac{\boldsymbol{x}_{,\xi}\,(\xi_c,\eta_c)\times\boldsymbol{x}_{,\eta}\,(\xi_c,\eta_c)}{\|\boldsymbol{x}_{,\xi}\,(\xi_c,\eta_c)\times\boldsymbol{x}_{,\eta}\,(\xi_c,\eta_c)\|}, \tag{9}$$

where $\boldsymbol{n}$ is the unit normal vector of the contact point $\boldsymbol{x}_c$.

When the penetration of the slave node is determined, the nodal contact force can be calculated using a penalty approach. Then, the nodal contact force for the slave node follows directly from its penetration. The nodal contact forces acting on the four master nodes, representing the master surface,

follow from the participation factors of the contact point according to the shape function and the contact point coordinates ξ_c and η_c.

For $g_n \leq 0$, there exists a contact. Following the penalty approach with a penalty parameter c_p, the nodal contact force can be determined as $f_c = c_p |g_n(\xi_c, \eta_c)|$, $g_n \leq 0$. The nodal contact force acting in the direction of the normal vector of the contact point can be calculated by $\boldsymbol{f}_c = \boldsymbol{n}(\xi_c, \eta_c) f_c$.

The nodal contact forces on the slave node and on the master nodes of a contact element finally follow as

$$\boldsymbol{f}_S = \boldsymbol{f}_c, \tag{10}$$

$$\boldsymbol{f}_{M,1} = -\frac{1}{4}(1+\xi_c)(1+\eta_c) f_c \boldsymbol{n}, \quad \boldsymbol{f}_{M,2} = -\frac{1}{4}(1-\xi_c)(1+\eta_c) f_c \boldsymbol{n}, \tag{11}$$

$$\boldsymbol{f}_{M,3} = -\frac{1}{4}(1-\xi_c)(1-\eta_c) f_c \boldsymbol{n}, \quad \boldsymbol{f}_{M,2} = -\frac{1}{4}(1+\xi_c)(1-\eta_c) f_c \boldsymbol{n}. \tag{12}$$

When all nodal contact forces are determined, the overall nodal contact force vector can be assembled and transformed to modal coordinates.

2.2. Simulation results

In this section, two involute gear pairs with parameters shown in Table 1 will be studied. The first pair is a straight gear pair, the other one is a helical gear pair. Both pairs have the same geometrical and material properties, except that the helical gears have a helical angle $\beta = 8°$.

Table 1.

Major design parameters of the gear pairs

	pinion	large gear
number of teeth	$z_1 = 18$	$z_2 = 37$
face width	$b_1 = 10$ mm	$b_2 = 10$ mm
root fillet radius	$\rho_{a1} = 0.25$ mm	$\rho_{a2} = 0.25$ mm
normal pressure angle	$\alpha_n = 20°$	
normal module	$m_n = 2$ mm	

As shown in [2] and [4], in a modally reduced elastic multibody model, the number of eigenmodes up to an eigenfrequency of about 80 kHz is necessary to get precise contact forces. In this study, the chosen number of eigenmodes will be checked to satisfy this requirement to get correct results. As integration scheme, an explicit Runge-Kutta scheme of order 4 with constant time step size is used.

For the contact calculation, all the teeth flanks of both gear pairs will be discretized very fine with the smallest finite element edge of about 0.06 mm for the straight gears and 0.063 mm for the helical gears. The straight gear model and the helical gear model consist of about 360000 and 406000 nodes, respectively, see Figure 3. The following results were obtained from the modally reduced elastic multibody model for both gear pairs. For precise results, for each pinion 200 eigenmodes and for each large gear 500 eigenmodes are used to fulfill the criterion stated above.

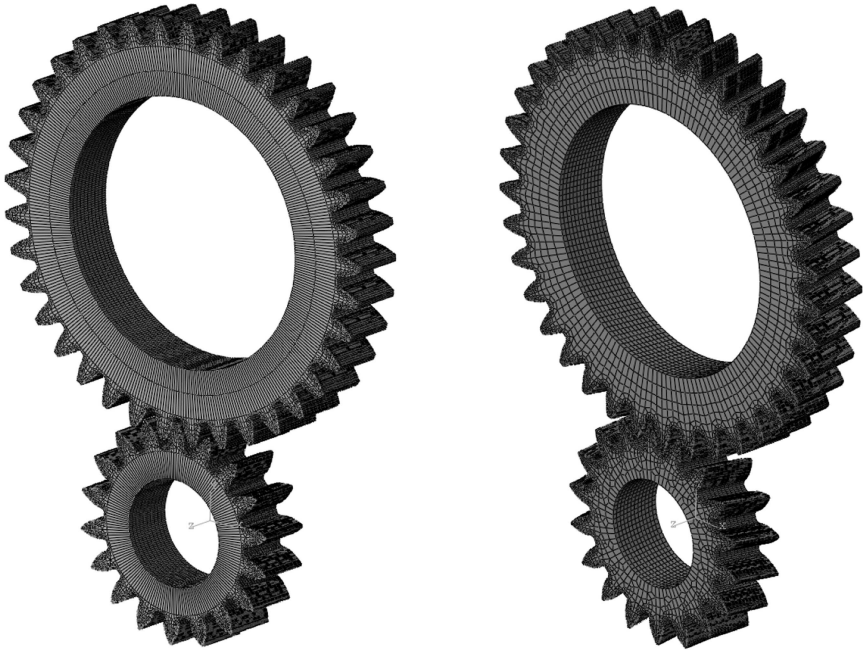

(a) (b)

Fig. 3. FE model of the straight gear pair (a) and of the helical gear pair (b)

Figure 4 presents simulation results of a few impacts of the helical gear pair. The pinion is given an initial rotational velocity of $\omega_0 = 50$ rad/s and the other gear is fixed. Figure 4(a) shows rotational velocities. The red and the blue lines describe the results of the FE model and of the elastic multibody model, respectively. The contact forces are shown in Figure 4(b). These contact forces are accumulated normal nodal contact forces of one flank. The impact results of the FE model and the elastic multibody model are in very good agreement with each other during the first three contacts. The contact forces of the two methods match very good in shape, magnitude and the number of teeth. The very small time shift between both models that can be observed from Figure 4(b) results from both models not being exactly the same, as one is a FE model and the other one is a reduced elastic

multibody model. Already a very small difference in mass results in a slightly different velocity after impact and, hence, a slightly later or sooner contact for the next impact. Obviously, this shift increases with increasing simulation time. However, this shift is very small and both models agree very well.

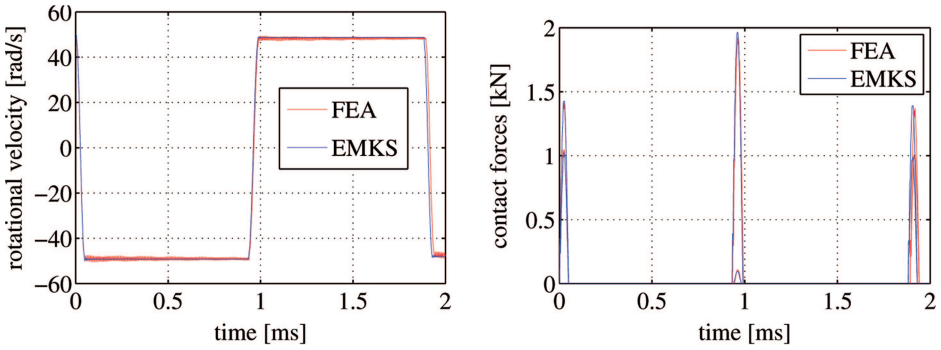

(a) (b)

Fig. 4. Rotational velocities (a) and contact forces (b) for the elastic multibody model and the FE model

As shown in [3] and [4], there are no difficulties for the simulation of large rotation angles or more revolutions of gears using this approach, even with very high rotational velocities of gear wheels. This is practically impossible for an FE analysis. Therefore, the following results are introduced only by the elastic multibody approach. Figures 5 and 6 introduce the contact forces of both gear pairs during meshing. Each color line describes an accumulated normal contact force period of one tooth pair.

Table 2.
Integration time, disk and memory requirement for impact investigations on the helical gear pair for 3 impacts for FE model and elastic multibody model using the same Computer (Intel Core i7-2600, 3.40GHz, 8 Cores and 32 GB RAM)

model	pre-processing (h)	integration time for 3 impacts (s)	disk requirement	memory requirement
FEM	0	71128	≈ 1.7 GB	≈ 1.7 GB
EMBS	20	1678	≈ 7 GB	≈ 1 GB

For each contact, some parts of the contact forces show a sudden change. The reason for these sudden changes is the so-called phenomenon of contact shock during meshing, when double-teeth contact changes to single-teeth contact and vice versa. The impacts produce noise, inaccuracy in the transmission ratio and wear, see [10]. This is particularly obvious for the straight gear pair, because theoretically the contact between teeth of this type of gears is more abrupt than of helical gears. Another reason for the sudden changes in

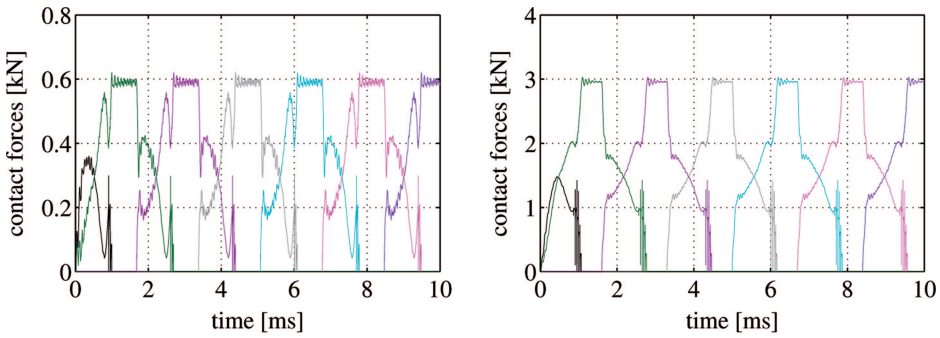

Fig. 5. Contact forces for the straight gear pair with a braking torque of 20 Nm (a) and 100 Nm (b) applied to the large gear

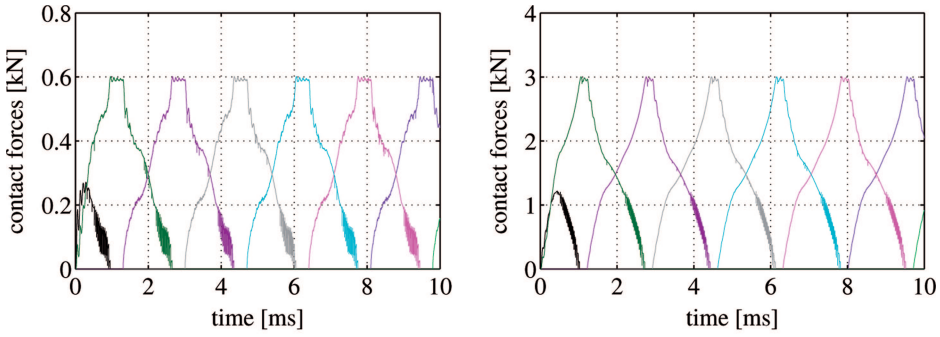

Fig. 6. Contact forces for the helical gear pair with a braking torque of 20 Nm (a) and 100 Nm (b) applied to the large gear

the contact forces is related to the transmitted load. As a result of the elasticity of the gears, a small bending of the teeth in contact occurs, causing a too early tip contact of the following teeth. This early contact is often accompanied by a very hard contact due to inappropriate contact geometries as a direct result of the tooth bending under load, see Figure 7(a). For the helical gear pair, the contact shock phenomenon is not so clear from the results, because theoretically the teeth of helical gears get into contact at a single point, and then, later go out of contact also at a point. In order to reduce the impact influence in industrial practice, particularly for straight gears, the involute profile in the tip region is most often modified, see Figure 7(b).

Both gear pairs are corrected by tip relief according to Figure 7(b) and the corrected gear pairs will be simulated with the same initial and boundary conditions as the uncorrected gear pairs. The results are shown in Figures 8, 9 and 10. Figure 8 shows the contact forces of the corrected straight gear pair, while Figure 9 presents the contact forces of the corrected helical gear pair.

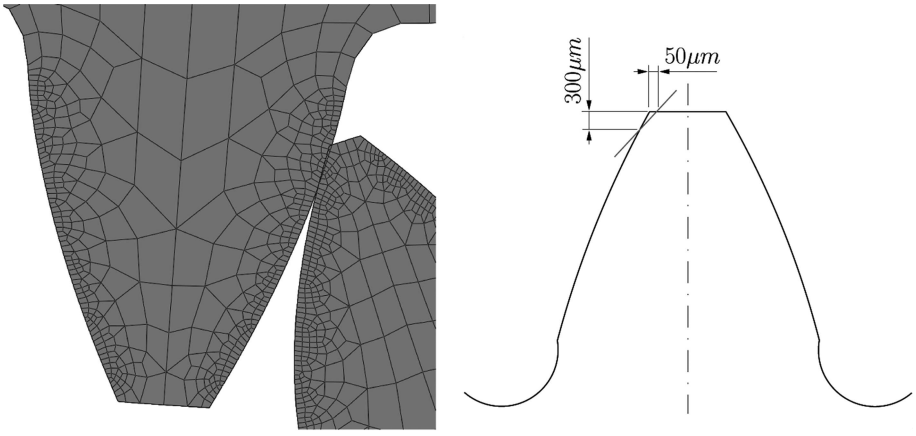

(a) (b)

Fig. 7. Change of contact geometry due to deformation under load (a) and flank profile correction by tip relief (b)

Again, each line describes the accumulated normal contact force of one tooth pair. Figure 10 presents an accumulated normal contact force of all tooth pairs in contact. For a perfectly steady operation this should be a perfectly horizontal line.

For the straight gear pair, comparing Figures 5 and 8, it can be seen that the contact shocks during meshing and the discontinuity of contact forces due to early tip contact are considerably reduced. This can also be seen from Figure 10, where the corrected gears show a much smoother line. A certain vibration of the contact forces still remains because of the elastic, dynamic and geometric effects, especially at the times where double-teeth contact changes to single-teeth contact and vice versa, but the overall contact behavior is tremendously enhanced by the tip relief.

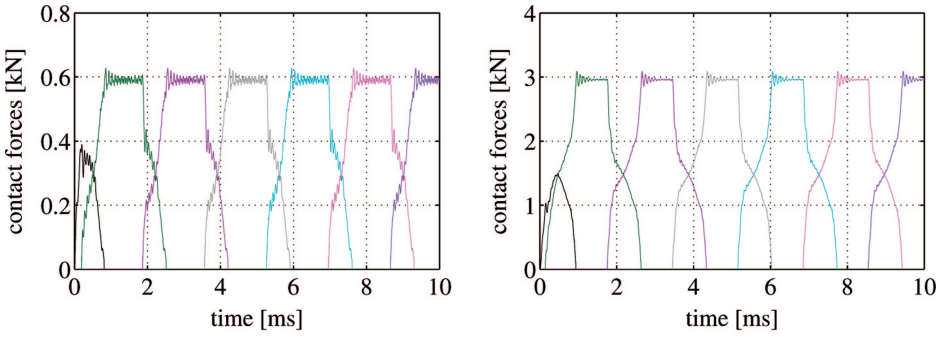

(a) (b)

Fig. 8. Contact forces for the corrected straight gear pair with a braking torque of 20 Nm (a) and 100 Nm (b) applied to the large gear

From Figures 6, 9 and 10(b), also for the helical gear pair, it can be observed that the contact shocks are reduced for the corrected gears. Again, the total contact force in Figure 10(b) shows the positive effect of the tip relief correction.

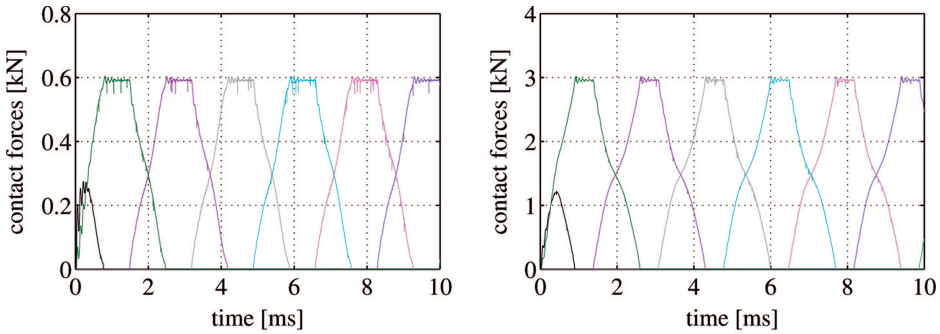

Fig. 9. Contact forces for the corrected helical gear pair with a braking torque of 20 Nm (a) and 100 Nm (b) applied to the large gear

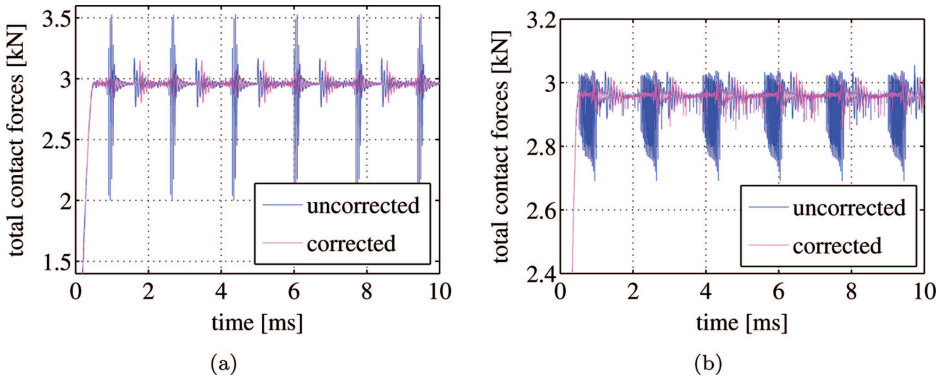

Fig. 10. Total contact forces for the straight gear pair (a) and the helical gear pair (b) with a braking torque of 100 Nm applied to the large gear

Another typical phenomenon of gear contact can be observed in Figures 8 and 9, namely that the duration of the single-teeth contact stages are inversely proportional to the applied forces on the gears because of deformation. When the applied forces increase, the elastic deformation of gear bodies also rises, and consequently the teeth will stay longer in contact. There is no difficulty to consider this phenomenon using the fully elastic approach. This is one of the advantages of the approach over a rigid body model, as the approach is fully elastic.

Another advantage of the approach is that a multistage of applied forces is quite simple to consider. Figure 11 and Figure 12 show the simulation

results of a multistage of applied forces with three different stages of driving torques of T_a = 100, 200 and 300 Nm applied to the large gears.

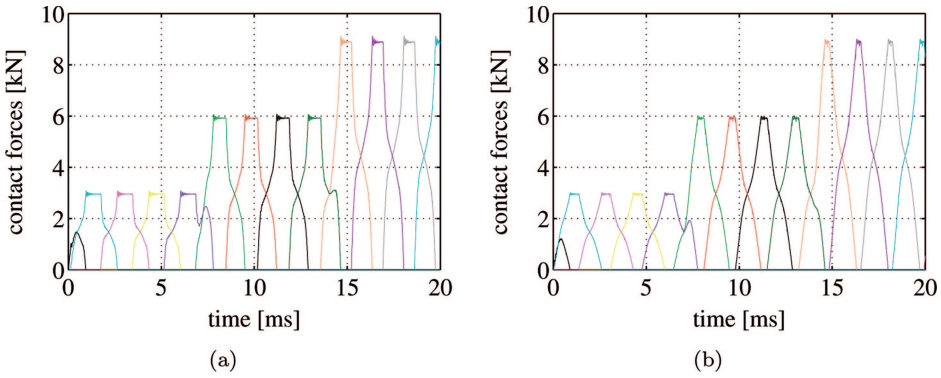

Fig. 11. Contact forces in a multistage of applied forces of the straight gear pair (a) and of the helical gear pair (b)

The consequence of the applied forces on the elastic deformation of the gear bodies and the contact-teeth stages are shown in Figure 11 and illustrate the increase in overlap with increasing driving torques. Figure 12 presents the consequence of the elastic deformation on the rotational velocity of the gears. The change in rotational velocity is directly proportional to the applied forces, and thus the deformations. With the same initial conditions and boundary conditions, because of the flank geometries, the effect of elastic deformation on the rotational velocity of the straight gears is much more significant than of the helical gears.

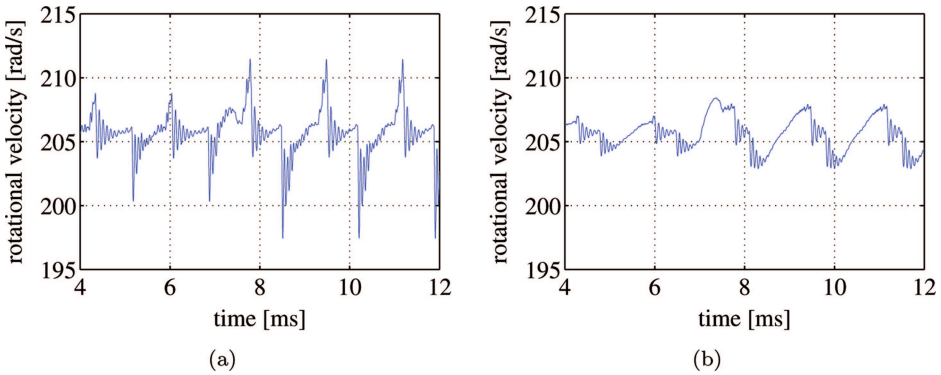

Fig. 12. Rotational velocities in a multistage of applied forces of the straight gear pair (a) and of the helical gear pair (a)

3. Beveloid Gear Pair

Theoretically, for rigid gears, the contact area of beveloid gear pairs under non-parallel axes meshing is point contact, see [11]. For flexible bodies, the contact area will enlarge to ellipses, but the contact ellipses are relatively small, and the tooth surface durability is generally low because of its high contact stress. In [9] the contact ellipses of two contact-teeth are computed using the commercial FE program Abaqus. The contact stress is presented and suggestions on how to solve problems associated with low-load capacity by enlarging the contact ellipses are also introduced. However, the simulation of the whole gear pair with large rotational angles or even full revolutions is still not practically feasible with FE. In this section, the fully elastic approach is applied to simulate the contact forces of the whole model of a straight beveloid gear pair.

3.1. Finite Element Model

The approach is applied to a straight beveloid gear pair. Both gears have a profile shift angle of $\theta = 10°$. The most important parameters are summarized in Table 3. The material used is steel with Young's modulus of $E = 2.1 \cdot 10^{11}$ N/m^2, density $\rho = 7850$ kg/m^3 and Poison ratio $\nu = 0.3$.

Table 3.

Major design parameters of the beveloid gear pair

	pinion	large gear
number of teeth	$z_1 = 19$	$z_2 = 38$
face width	$b_1 = 20$ mm	$b_2 = 20$ mm
profile offset in the middle of tooth	0	0
profile shifting angle	$\theta_1 = 10°$	$\rho_2 = 10°$
helical angle	$\beta_1 = 0°$	$\beta_2 = 0°$
root fillet radius	$\rho_{fP1} = 0.25$ mm	$\rho_{fP2} = 0.25$ mm
normal pressure angle	$\alpha_n = 20°$	
normal module	$m_n = 2$ mm	
intersected angle of shafts	$\Sigma = 20°$	
head clearance factor	$c_a = 0.2$ mm	

Again, the flanks are specially discretized very fine. Since the flank profiles are highly complex, in order to describe the flank geometry precisely, the teeth must be discretized fine enough in both directions of the flank, the flank width and the face width. The FE model of the beveloid gear pair consists

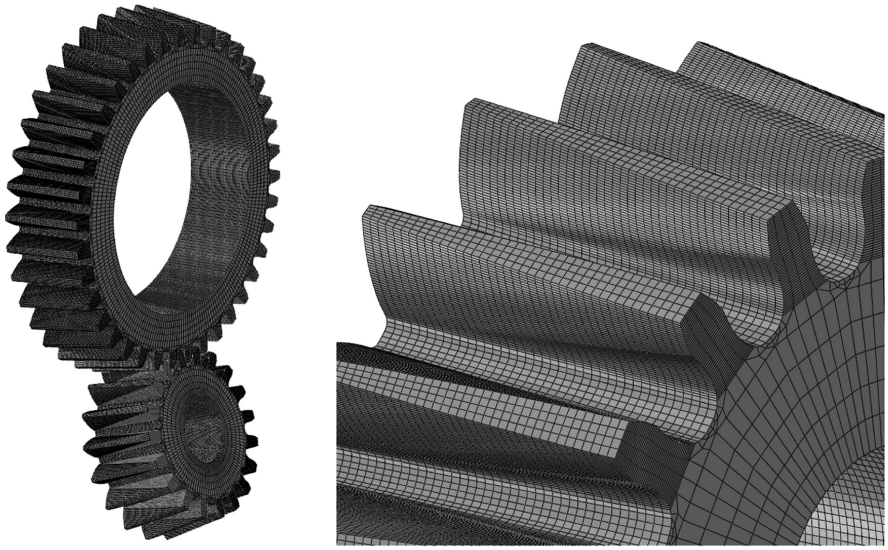

(a) (b)

Fig. 13. The straight beveloid gear pair (a) with non-standard flank profiles (b)

of about 303000 nodes and 250000 elements, with a smallest element edge in the contact areas of about 0.13 mm. A linear hexahedral element with reduced integration is used here.

3.2. Simulation results

The following results are obtained from the modally reduced elastic multibody model for the beveloid gear pair. The pinion is given an initial rotational velocity of $\omega_0 = 50$ rad/s and a braking torque of $T_a = 1000$ Nm is applied to the large gear. For both the pinion and the large gear, 1000 eigenmodes are used for the reduced model. Simulated contact forces of the gear pair are presented in Figure 14, where each color line is a contact force of one tooth pair. During the whole simulation, there are always two tooth pairs in contact at the same time, see Figure 14(a). Figure 14(b) shows the change of the rotational velocity, caused by the elastic deformation and the complex flank form.

Figure 15 presents the simulation results of the beveloid gear pair but for a higher rotational velocity of about $\omega_0 = 200$ rad/s for the pinion. The boundary conditions and the braking torque are the same as in the previous simulation. Figure 15(b) presents the contact forces. Again, there are always two tooth pairs in contact at the same time. Figure 15(b) shows that the effects of the elasticity and the complex flank form are directly related to the speed of gear wheels.

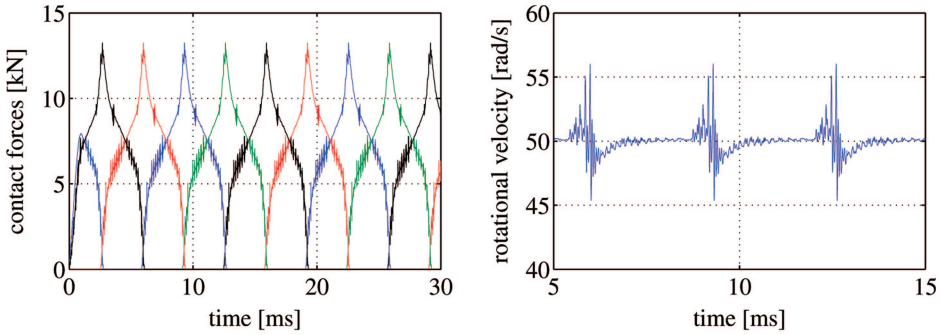

(a) (b)

Fig. 14. Contact forces (a) and rotational velocity (b) of the model with low initial rotational velocity

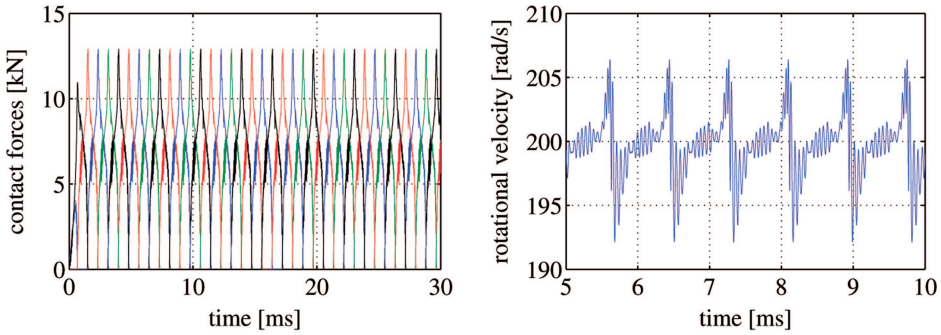

(a) (b)

Fig. 15. Contact forces (a) and rotational velocity (b) of the model with higher initial rotational velocity

Figure 16 shows the contact area during meshing of a tooth pair. The data on which the figure is based, is acquired directly from the contact calculation process during the simulation. The figure describes the pinion in red and the large gear in green.

As mentioned in Section 2, the contact between two flanks will be described using a master/slave contact element. The blue nodes in Figure 16 are the master nodes of the flank pair in contact. These points describe approximately the contact area of the contact. Together with the nodal contact forces available from the contact forces calculation, this would allow to estimate and illustrate the contact pressure in the contact patch.

For beveloid gears, the contact ellipses are relatively small, leading to low-load capacity of the gear pair. Figure 16(a) shows the contact area in the case of an applied torque of T_a = 2500 Nm, and Figure 16(b) corresponds to an unrealistically high of the applied torque, of T_a = 10000 Nm, on the large

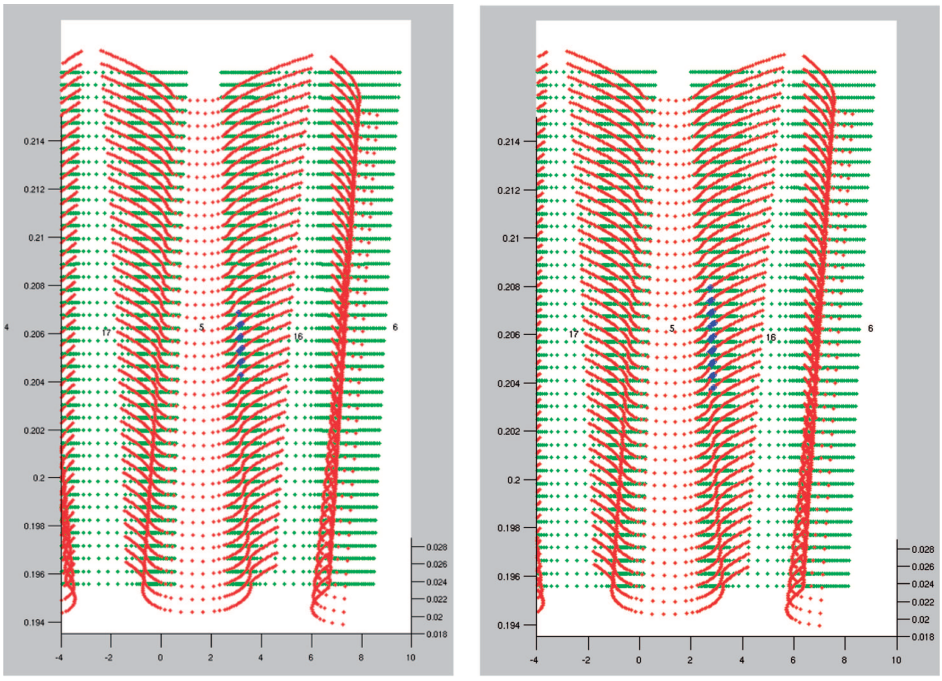

(a) (b)

Fig. 16. Contact area of gear teeth with high applied forces (a) and very high applied forces (b)

gear wheel. The results show that the contact ellipse is enlarged following the increase of applied forces, but is still rather small.

4. Conclusion

In this study, a very detailed nonlinear FE model with contact and an elastic multibody model of a helical gear pair has been used to investigate several impacts. The simulation results of the two approaches agree very well. The time integration of the elastic multibody approach is much more efficient than a fully nonlinear transient FE analysis.

The work also shows how the modal approach can be used to efficiently investigate the interaction between elastic deformations and flank profile corrections as well as their influence on the contact forces and their rotational velocities. Two very detailed gear pair models, one straight gear pair and one helical gear pair, were modeled to simulate the contact forces in dependence of the transmitted load. Some interesting phenomena of spur gears were observed that are automatically included in the fully elastic approach as opposed to classical approaches with rigid body models.

This approach allows precise investigations of contacts between gears with almost arbitrary non-standard tooth geometries or flank profile correc-

tions. Even precise simulations of gears with flank profiles as complex as the investigated beveloid gears are possible and simulation results are shown.

Manuscript received by Editorial Board, October 11, 2012;
final version, January 10, 2013.

REFERENCES

[1] Bauchau O.A.: Flexible Multibody Dynamics. Dordrecht: Springer, 2011.
[2] Ziegler P., Eberhard P.: Simulative and Experimental Investigation of Impacts on Gear Wheels. Computer Methods in Applied Mechanics and Engineering, Vol. 197, No. 51-52, pp. 4653-4662, 2008.
[3] Ziegler P., Eberhard P.: Investigations of Gears Using an Elastic Multibody Model with Contact. Multibody Dynamics: Computational Methods and Applications, W. Blajer, K. Arczewski, J. Fraczek, and M. Wojtyra (eds.), 2010.
[4] Ziegler P.: Dynamische Simulation von Zahnradkontakten mit elastischen Modellen. Dissertation, Schiften aus dem Institut für Technische und Numerische Mechanik der Universität Stuttgart, Band 23. Shaker Verlag, Aachen, 2012.
[5] Tamarozzi T., Ziegler P., Eberhard P., Desmet W.: On the Applicability of Static Modes Switching in Gear Contact. The 2nd Joint International Conference on Multibody Dynamics, May 29-June 1, 2012, Stuttgart, Germany.
[6] Sherif K., Witteveen W., Mayrhofer K.: Quasi-Static Consideration of High-Frequency Modes for More Efficient Flexible Multibody Simulations. Acta Mech 223, 1285-1305, Springer-Verlag, 2012.
[7] Wang S.P., Nakamachi E.: The Inside-Outside Contact Search Algorithm for Finite Element Analysis. International Journal for Numerical Methods in Engineering, Vol. 40, pp. 3665-3685, 1996.
[8] Chen Y.-C., Liu C.-C.: Contact Stress Analysis of Concave Conical Involute Gear Pairs with Non-Parallel Axes. Finite Elements in Analysis and Design, Vol. 47, pp. 443-452, 2011.
[9] Liu C.-C., Tsay C.-B.: Mathematical Models and Contact Simulations of Concave Beveloid Gears. Journal of Mechanical Design, Vol. 124, pp. 753-760, 2002.
[10] Liu C.-C., Chen Y.-C., Lin S.-H.: Contact Stress Analysis of Straight Concave Conical Involute Gear Pairs with Small Intersected Angles. Proceedings of the International MultiConference of Engineers and Computer Scientists 2010, Vol. III, IMECS, Hong Kong, March 17-19, 2010.
[11] Liu C.-C., Tsay C.-B.: Contact Characteristics of Beveloid Gears. Mechanism and Machine Theory, Vol. 37, pp. 333-350, 2002.
[12] Markovic K., Franulovic M.: Contact Stresses in Gear Teeth Due to Tip Relief Profile Modification, Engineering Review, Vol. 31-1, pp. 19-26, 2011.
[13] Brecher C., Röthlingshöfer T., Gorgels C.: Manufacturing Simulation of Beveloid Gears for The Use in a General Tooth Contact Analysis Software. Production Engineering Research and Development, Vol. 3, pp. 103-109, 2009.
[14] Zhu C., Song C., Lim T.-C., Vijayakar S.: Geometry Design and Tooth Contact Analysis Crossed Beveloid Gears for Marine Transmissions. Chinese Journal of Mechanical Engineering, Vol. 24, No. 5, 2011.
[15] Shabana A.A.: Dynamics of Multibody Systems. University Press, Cambridge, 1998.
[16] Schwertassek R., Wallrapp O.: Dynamik flexibler Mehrkörpersysteme (in German). Vieweg, Braunschweig, 1999.

[17] Lehner M., Eberhard P.: A Two-Step Approach for Model Reduction in Flexible Multibody Dynamics. (Special Issue Realtime, Ed. J. Cuadrado). Multibody System Dynamics, Vol. 17, No. 2-3, pp. 157-176, 2007.
[18] Eberhard P., Fehr J., Mathuni S.: Influence of Model Reduction Techniques on the Impact Force Calculation of Two Flexible Bodies. PAMM, Vol. 9, pp. 111-112, 2009.
[19] Fehr J., Eberhard P.: Simulation Process of Flexible Multibody Systems with Advanced Model Order Reduction Techniques. Multibody System Dynamics, Vol. 25, No. 3, pp. 313-334, 2011.

Symulacja sprężystej przekładni zębatej o niestandardowych profilach powierzchni bocznych zębów

S t r e s z c z e n i e

Istnieją przypadki, gdy dla dokładnej symulacji sił kontaktowych nie można modelować kół zębatych jako ciał sztywnych, lecz jest potrzebny opis w pełni sprężysty. W artykule zaproponowano model systemu wielu ciał uwzględniający styki między zębami, modalnie zredukowany i z zastosowaniem układu odniesienia o płynnych ramach, umożliwiający bardzo dokładną symulację w pełni sprężystych kół zębatych o różnych rodzajach zazębienia. Symulacja jest możliwa dla znacznej liczby obrotów, przy czym wymagany czas obliczeń jest stosunkowo krótki. Zaletą tego podejścia jest, że nie wymaga ono założeń co to geometrii zębów, dzięki czemu można dokładnie badać zjawiska na stykach między zębami dla dowolnych, niestandardowych geometrii zębów, w tym również o skorygowanym profilu powierzchni bocznej.

W artykule przedstawiono wyniki symulacji, które pokazują, że takie modalne podejście może być użyteczne przy badaniu zależności między odkształceniami sprężystymi a korekcją profili zębów, a także ich wpływu na siły kontaktowe. Pokazano, że stosując model sprężysty można opisywać ważne zjawiska, takie jak wczesny kontakt głowy zęba w przypadku niedostatecznej korekcji profilu w zależności od przenoszonego obciążenia. Co więcej, pokazano że opisany sposób podejścia może być wykorzystany przy precyzyjnej i wydajnej symulacji przekładni stożkowych.